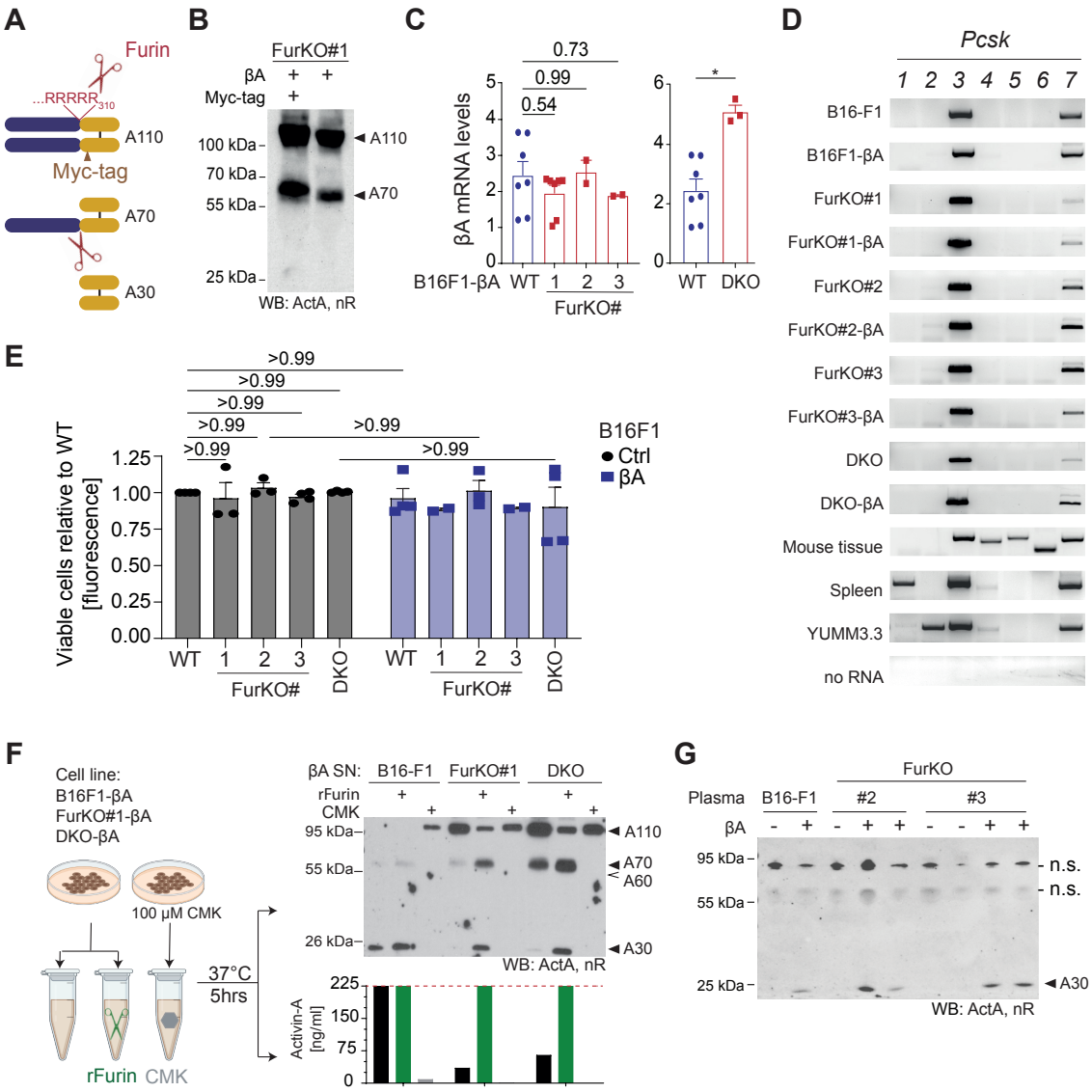

Supplementary figure S1. Analysis of *INHBA* and *Pcsk* mRNA expression in stably transduced B16-F1 cell lines, and of Activin-A protein in plasma of tumor-bearing mice.

(A) Schematic representation of Activin-A processing. Cleavage of one or both βA subunits of proActivin-A (A110) by furin at the S1 site gives rise to half-processed (A70) or fully mature Activin-A (A30), respectively [27].

(B) Comparison of Activin-A with or without a myc epitope tag in SN of transfected FurKO#1 cells.

(C) RT-qPCR analysis of βA transcripts normalized to endogenous *Gapdh* mRNA in βA-transduced B16-F1 cell lines of the indicated *Furin* genotype. WT, wild-type; FurKO, Furin knock-out; DKO, *Furin* and *Pcsk7* knock-out. Data represent means ± SEM (n = 2-7 per group); *p<0.05, Student's t-test.

(D) RT-PCR analysis of *Pcsk1* (PC1), *Pcsk2* (PC2), *Pcsk3* (Furin), *Pcsk4* (PC4), *Pcsk5* (PC5/6), *Pcsk6* (PACE4), and *Pcsk7* (PC7) mRNAs in parental B16-F1 melanoma cells and CRISPR/Cas9-edited FurKO and DKO clones before and after lentiviral transduction with *INHBA* (βA), in YUMM3.3 cells, and in total RNA from spleen or tissue pooled from multiple organs of a 10-week-old female C57BL/6J mouse.

(E) Proliferation of empty lentivirus-transduced B16-F1 cells (Ctrl) and of the cell lines in (B) analyzed by Alamar Blue assay. Error bars, SEM (n = 2 to 3 independent experiments); *p<0.05, **p<0.01, ***p<0.001, ****p<0.0001, ordinary one-way ANOVA with Šídák's multiple comparisons test.

(F) Left: Evaluation of the specificity of an ELISA kit for mature Activin-A in B16F1-βA, FurKO#1-βA, or DKO-βA cells (schema was created using BioRender.com). SNs of CMK-treated cells were used to assess the reactivity of the ELISA kit with uncleaved A110. Where indicated, SNs of cells without CMK were treated with recombinant furin during 5 hrs. Right: Western blot analysis on non-reducing gels served to validate Activin-A processing and its inhibition by CMK treatment (top right panel). Activin-A concentrations measured by ELISA in the same samples are shown below the blot. Note that while all values for samples containing A30 were beyond the dynamic range of the assay (stippled line), the reactivity of samples containing mainly A100 with or without A70 was minimal or below detection, respectively, indicating that the ELISA kit detects mature Activin-A but not half-processed or uncleaved forms.

(G) Activin-A Western blot of plasma from tumor-bearing mice collected at the endpoint.

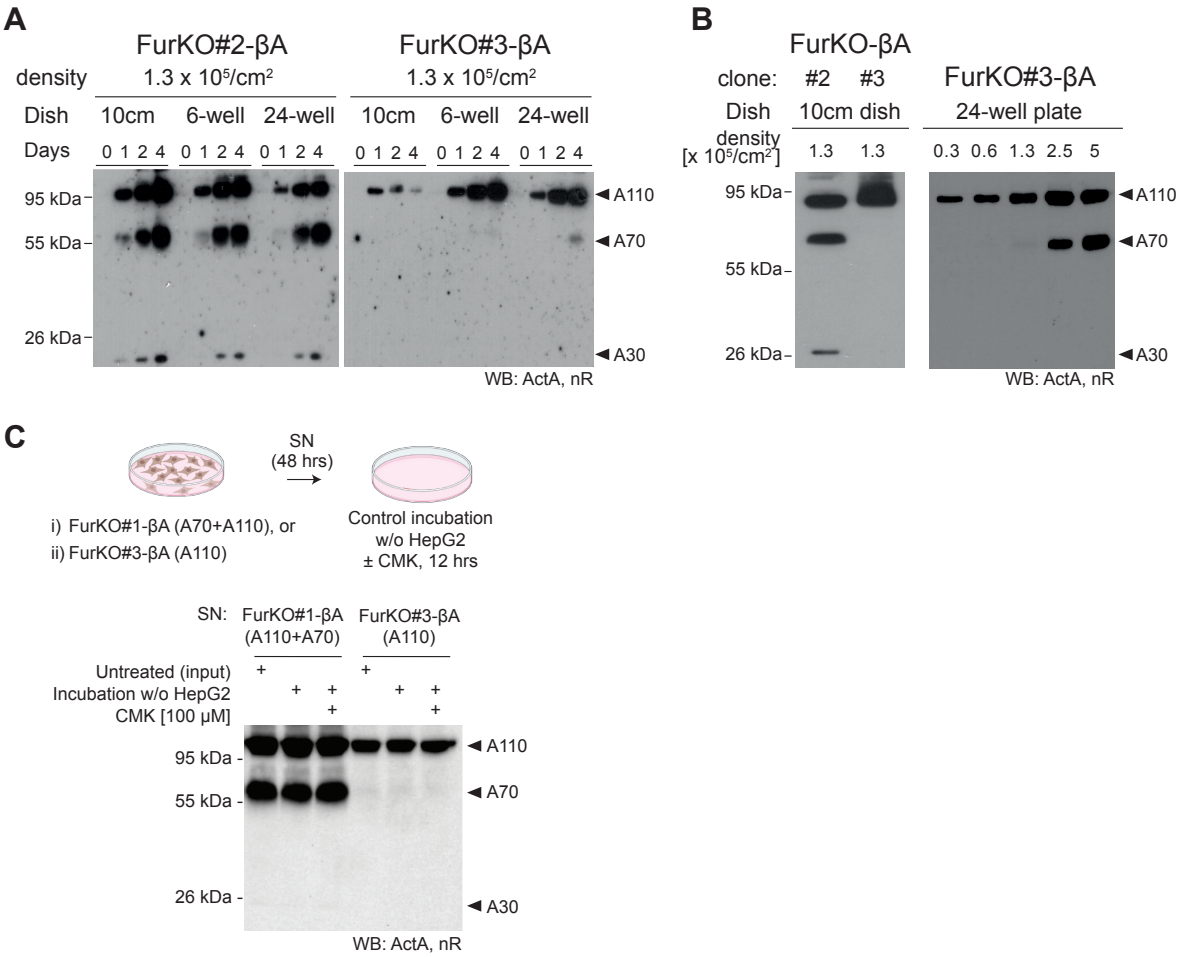

Supplementary figure S2. Influence of cell density on the furin-independent PCLP cleavage of Activin-A by FurKO#2 versus FurKO#3 cells.

(A) Western blot analysis of Activin-A in cell SNs of βA-transduced FurKO clones #2 and #3 seeded at a density of 1.3 x 10^5 cells/cm^2 and incubated for up to 4 days in the indicated type of tissue culture dishes. Note the inhibition of A70 formation in FurKO#3-βA cells that have not reached confluence.

(B) Western blots of SNs from FurKO#2-βA and FurKO#3-βA cell lines in 10 cm dishes (left) and of FurKO#3-βA cells in 24-well plates 48 hrs after cell seeding at the indicated density (right). Note the rescue of A70 formation in FurKO#-βA cells at confluent cell density.

(C) Western blot analysis of Activin-A processing after control incubation of the indicated cell SNs for 12 hrs at 37 ºC without HepG2 CAGA-Luc reporter cells. Schema was created using BioRender.com.

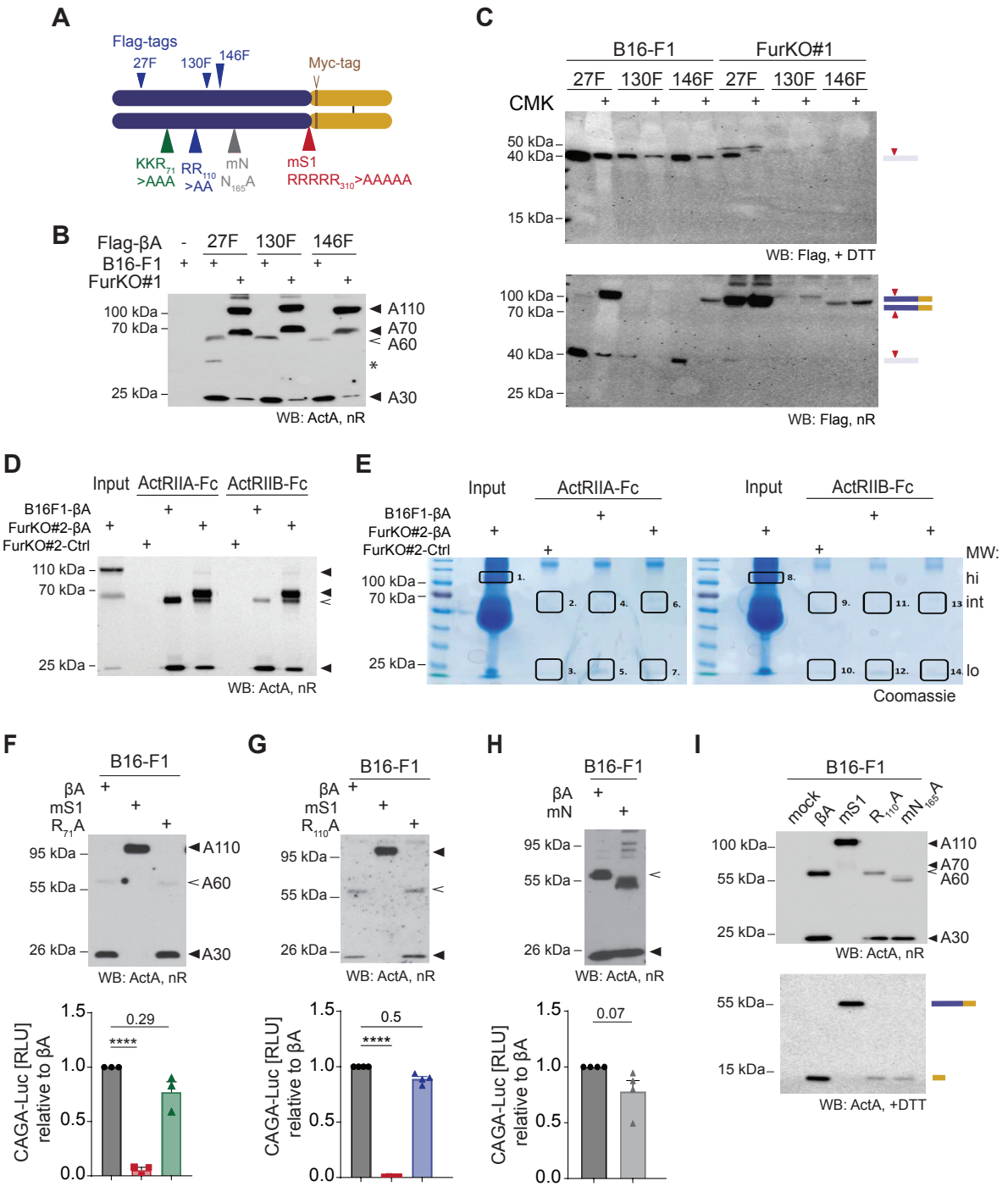

Supplementary figure S3. Analysis of the Activin-A prodomain by tagging it with a Flag epitope, or by mutating either dibasic motifs or the N-glycosylation site.

(A) Schema of the myc-tagged Activin-A precursor dimer. Arrowheads highlight alternative positions after which we inserted a Flag epitope (E27, G130, or D146). The mutated N-glycosylation site N165 (mN), and sequences of the mutated S1 cleavage site (mS1) and of the dibasic motifs RR_{110} and KKR_{71} that were substituted by alanines are shown below.

(B) Representative non-reducing anti-Activin-A Western blot of SNs from B16-F1 or FurKO#1 cells transfected with the indicated Flag-tagged βA constructs. Note that a Flag tag at position 27 stabilized traces of an additional 40 kDa fragment reacting with anti-Activin-A antibody (asterisk).

(C) As in (B) but SNs collected from cells treated or not with 100 μM CMK and analyzed by reducing (top) or non-reducing (bottom) anti-Flag Western blot.

(D) Pull-down of Activin-A from 10-fold concentrated SNs of B16F1-βA or FurKO#2-βA cells by Fc fusions of the extracellular domains of ActR-IIA or ActR-IIB, analyzed by Western blot.

(E) Coomassie staining of preparative gels loaded as in (D) to excise regions of interest (rectangles) containing Activin-A isoforms in the high (H), intermediate (I) or low (L) molecular weight range for liquid chromatography-mass spectrometry (LC-MS) analysis. Gel-purified A110 from the input, or pull-downs from FurKO#2-Ctrl SNs served as positive and negative controls, respectively.

(F-H) Anti-Activin-A Western blot of SNs from B16-F1 cells transfected with βA or with the indicated mutant derivatives. Induction of CAGA-Luc in HepG2 reporter cells by these same SNs is shown below). Error bars, SEM (n = 3 or 4 independent experiments); *p<0.05, **p<0.01, ***p<0.001, ****p<0.0001, Student's t-test.

(I) Western blot analysis of Activin-A under non-reducing (top) or reducing conditions (bottom) in SN of B16-F1 cells transfected with the indicated βA constructs.

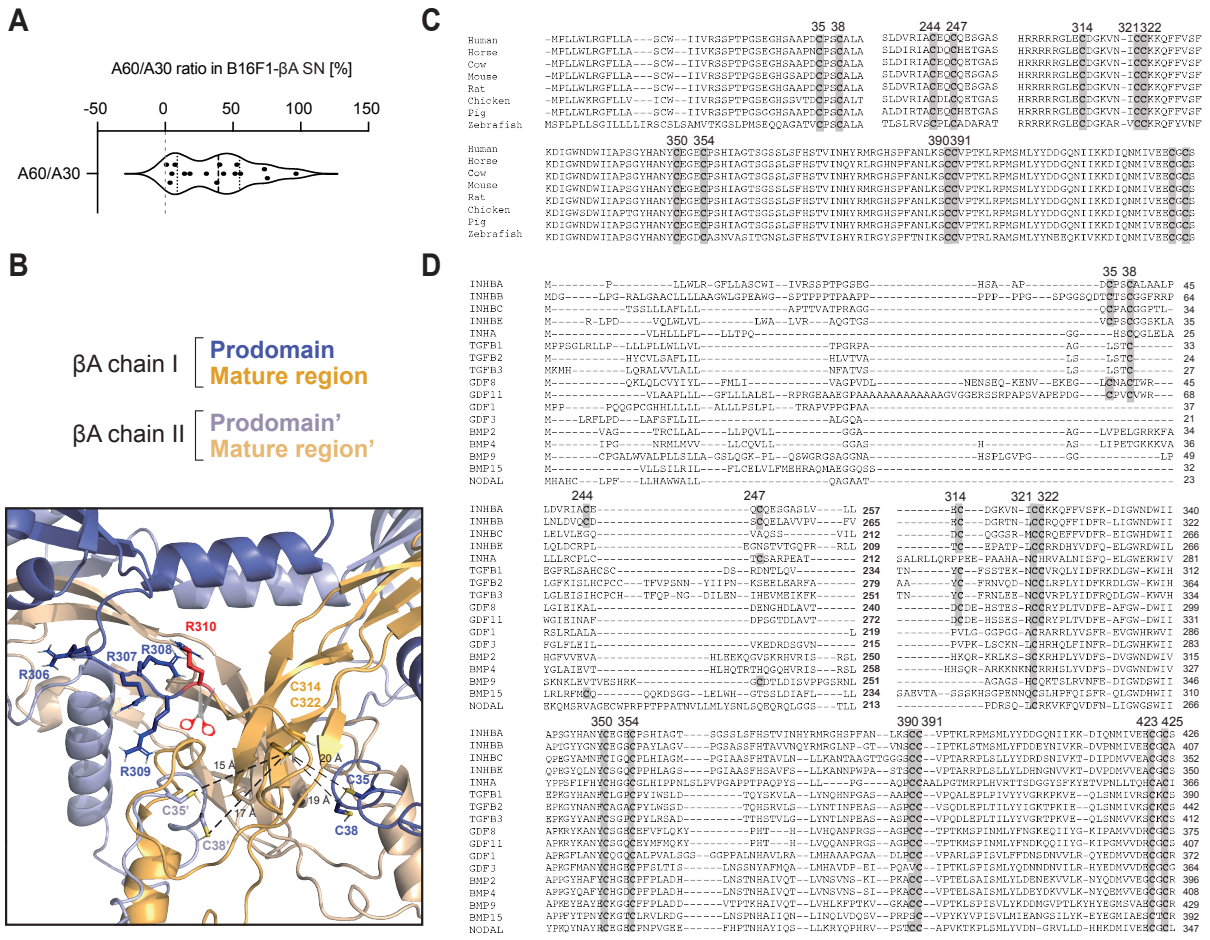

Supplementary figure S4. Conservation of cysteines in proActivin-A and their role in regulating A60 formation

(A) Variability in the ratio of A60 relative to A30 in B16F1-βA cell SN (n = 16 unrelated experiments).

(B) Positioning of a known disulfide between C314 and C322 in the mature region (orange) relative to C35 and C38 in the prodomain (violet) that is predicted by AlphaFold based on the proActivin-A crystal structure (PDB: 5HLZ). Distances between the sulfur atoms of C322 and C35 of the same βA chain (19-20 Å) or of the other subunit (15-17 Å) are indicated by stippled lines.

(C, D) Sequence alignments of (C) INHBA genes from the indicated species, and (D) of human INHBA with other representative TGF-β family members. Conserved cysteines are highlighted in gray.

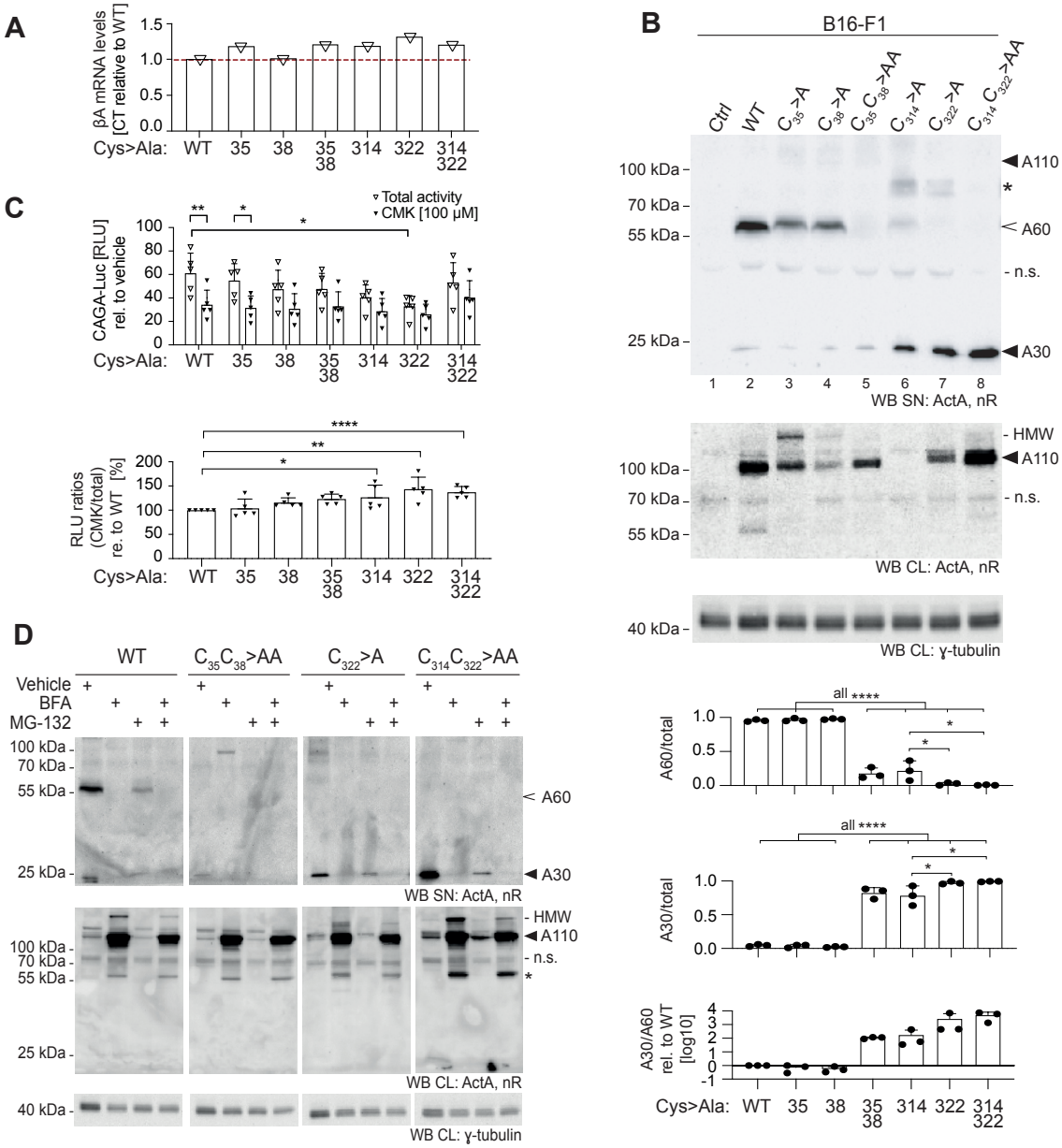

Supplementary figure S5. Effects of cysteine mutations on Activin-A processing in stably transduced B16-F1 melanoma cell lines.

(A) RT-qPCR analysis of myc*INHBA* mRNA levels normalized to endogenous *Gapdh* mRNA in B16-F1 cells expressing the indicated cysteine mutant βA, relative to wild-type (WT) control.

(B) Anti-Activin-A Western blots of extracts (CL) from the B16-F1 cell lines indicated at the top, and of their culture medium after 48 hrs of conditioning (SN). Proteins were denaturated with SDS and separated on a non-reducing gel to preserve the cysteine bonds (n = 3 experiments).

(C) Relative luciferase units (RLU) induced in HepG2 CAGA-Luc reporter cells in the presence of 100 μM CMK or empty vehicle (total activity) after 12 hrs treatment with 1:10 diluted SNs of B16F1 cell lines stably expressing WT βA, or the indicated cysteine mutants, normalized to the baseline. Note that …. Error bars, SD (n = 5 independent experiments), two-way ANOVA.

(D) Non-reducing anti-Activin-A Western blot analysis of SNs and lysates (CL) from B16-F1 cells stably expressing WT-βA, or the indicated cysteine mutants. Where indicated, cells were treated with 5 μg/mL brefeldin A (BFA) or with 10 μM MG-132, or both. HMW: high molecular weight complex; n.s.: non-specific band; asterisk (61 kDa): Possible breakdown product (n = 3 experiments).

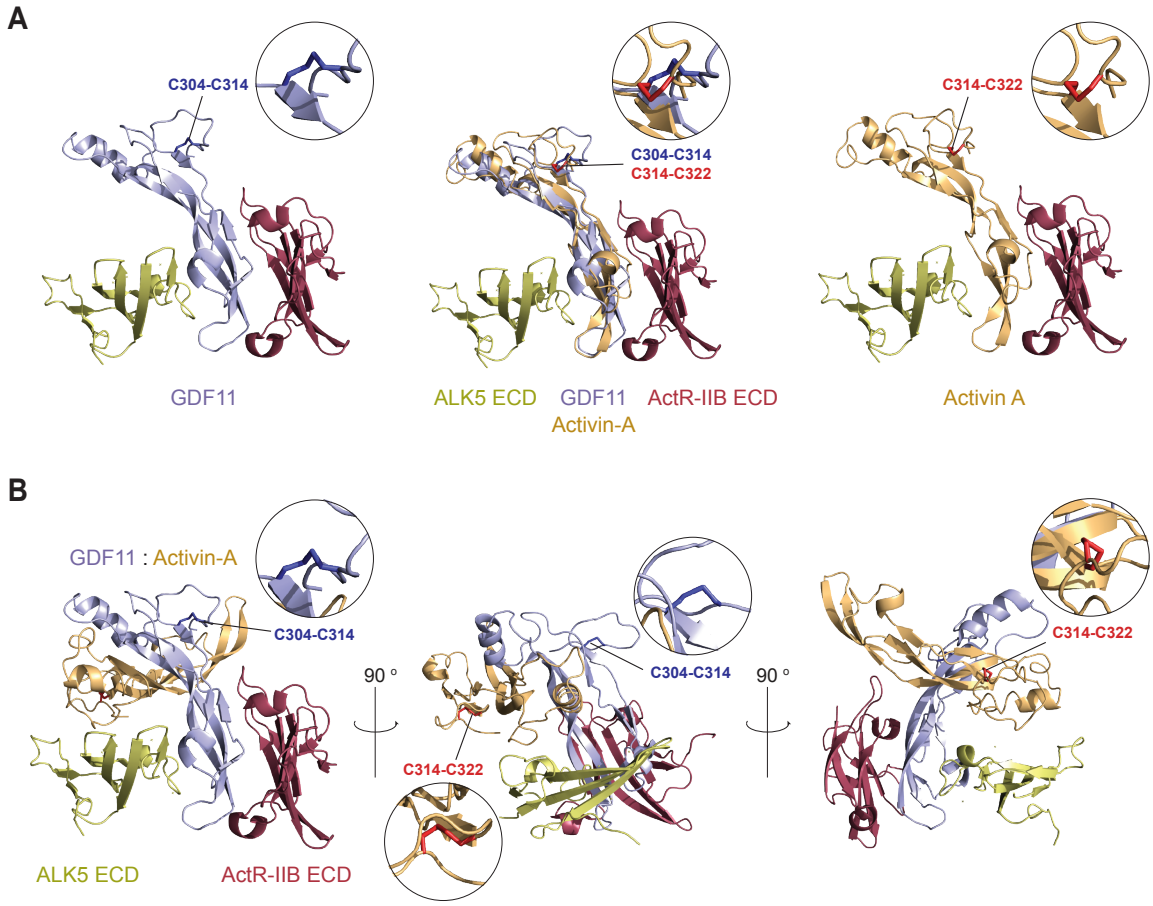

Supplementary figure S6. Position of cysteines C314 and C322 relative to signaling receptors predicted by structural modeling.

(A) Crystal structure of one subunit of mature Activin-A (orange) superimposed on the known structure of one monomeric subunit of the related GDF11 (lilac) in complex with the extracellular domains (ECD) of its type I receptor ALK5 (green) and of ActR-IIB (red).

(B) As in (A), but with artificial dimer of one subunit of GDF11 and one Activin-A subunit.

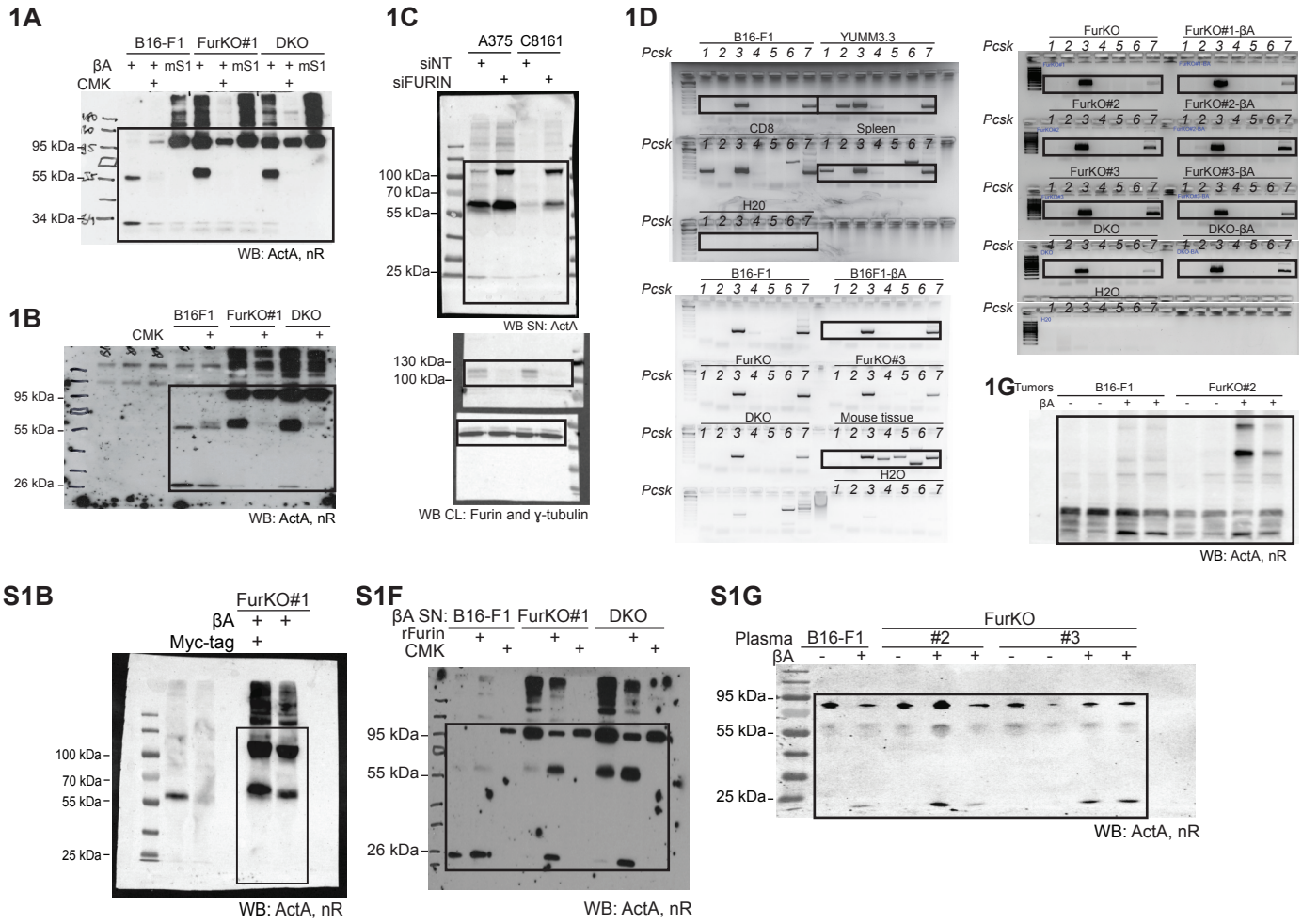

Supplementary figure S7. Source data "uncropped images".
Boxed areas are shown in the corresponding panels of the figures indicated.

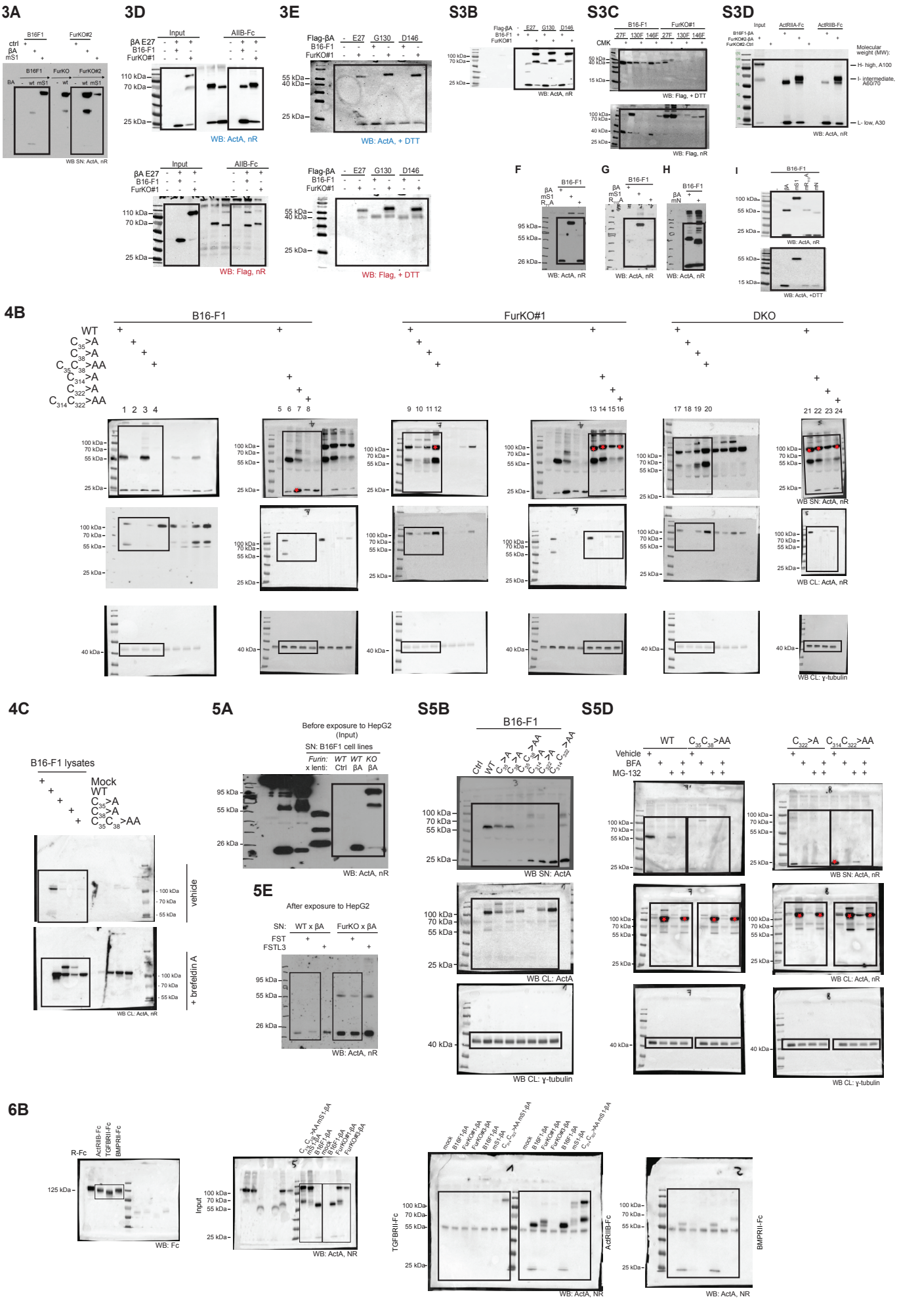

Supplementary figure S7 (continued). Source data "uncropped images".
Boxed areas are shown in the corresponding panels of the figures indicated.

Supplementary Table S1. RT-(q)PCR primers

Gene		Primer sequence
mycINHBA	fw	CCGAGGAGGACCTGTGTGA
	rev	ATCCAGTCATTCCAGCCGATG
PC1/*Pcsk1*	fw	TGATGATCGTGTGACGTGGG
	rev	CACTCCAAGCCATCATCCAGT
PC2/*Pcsk2*	fw	ACAGCCCCACTTTTCACTCC
	rev	CAAAGGGGAGCTTTCGGACT
Furin/*Pcsk3*	fw	TCCCCAGGATCTGGCCCTTA
	rev	CGACCACCCATAGCAACCAG
PC4/*Pcsk4*	fw	ACCCTGGGCCTGGAGAATAA
	rev	GAGGGGACTGTGACTTTCCTG
PC5(6)/*Pcsk5*	fw	CCCGTAACAAGGGTCTTGGA
	rev	TCCCTTGGCAGGATAATGGC
PACE4/*Pcsk6*	fw	CGGAAGATCGTCACCACAGA
	rev	TTTATGCCCAGCTCCGTTGA
PC7/*Pcsk7*	fw	CGAGAGTTTCCGTAGGGTGG
	rev	CATCAGAACAGCAGGCTGGG

Supplementary Table S2. OE-PCR primers used to generate the indicated mutant βA constructs

Construct		Mutagenic primer sequence
mS1	fw	GCGGCCGCCGCAGCTGGCTTGGAGCAGAAGCTG
	rev	AGCTGCGGCGGCCGCATGAGGGTGGTCTTCAGAC
mS2	fw	GGATGACATTGGAGCGGCGGCAGAAATGAA
	rev	TTCATTTCTGCCGCCGCTCCAATGTCATCC
mS2'	fw	CATGCTGCACTTGGCGGCGGCGCCCGATGTC
	rev	GACATCGGGCGCCGCCGCCAAGTGCAGCATG
mN	fw	GTCCCCAAGGCCGCGAGGACCAGGACC
	rev	GGTCCTGGTCCTCGCGGCCTTGGGGAC
E27-Flag	fw	CAAAGACGATGACGACAAGGGGCACAGCGC
	rev	GTCATCGTCTTTGTAGTCCTCGGATCCTGG
G130-Flag	fw	ACAAAGACGATGACGACAAATCGGGAACAGCCAGGAAG
	rev	GTCGTCATCGTCTTTGTAGTCTCCTGACTCGGCAAACG
D146-Flag	fw	ACTACAAAGACGATGACGACAAGGGCTCAGTGGTGGAG
	rev	GTCATCGTCTTTGTAGTCTGAGCCGTCACTGCCTTCCTTG
C35A	fw	CGACGCTCCGTCCTGTGCGCTGGCCGCCC
	rev	CCAGCGCACAGGACGGAGCGTCGGGGGCC
C35C38AA *	fw	CGACGCTCCGTCCGCGGCGCTGGCCGCCC
	rev	GGGCGGCCAGCGCCGCGGACGGAGCGTCG
C314A	fw	GGACCTGGCTGATGGCAAGGTC
	rev	CCTTGCCATCAGCCAGGTCCTC
C322A	fw	GTCAACATCTGCGCTAAGAAACAGTTC
	rev	GAACTGTTTCTTAGCGCAGATGTTGACC
C314C322AA	fw	GGACCTGGCTGATGGCAAGGTCAACATCTGCGCTAAGAAAC
	rev	GTTTCTTAGCGCAGATGTTGACCTTGCCATCAGCCAGGTCCTC

* C38A was obtained from an OE-PCR clone where only C38 happened to be mutated by this primer